

PSI ‘Neutron Microscope’ at ILL-D50 Beamline - First Results

Pavel Trtik^{1, a*}, Michael Meyer¹, Timon Wehmann¹, Alessandro Tengattini^{2,3},
Duncan Atkins³, E.H. Lehmann¹, Markus Strobl¹

¹Paul Scherrer Institut (PSI), Laboratory for Neutron Scattering and Imaging, CH-5232 Villigen PSI, Switzerland

²Université Grenoble Alpes (UGA), CNRS, Grenoble INP, 3SR, Grenoble 38000, France

³Institut Laue-Langevin (ILL), 71 Avenue des Martyrs, Grenoble 38000, France

^a pavel.trtik@psi.ch

*corresponding author: Pavel Trtik (PSI)

Keywords: Neutron, Microscope, High-Resolution Neutron Imaging, Cold Neutrons, Beam Intensity

Abstract. A high-resolution neutron imaging system referred to as ‘Neutron Microscope’ (NM) has been recently established as a piece of instrumental equipment at the Paul Scherrer Institut (PSI), Switzerland. It is providing the wide user community of the Neutron Imaging and Applied Materials Group (NIAG) with the capability of spatial image resolution below 5 μm at effective pixel sizes of 1.3 μm. The NM has been designed as a portable, self-contained system that can be moved between beamlines at PSI with only moderate effort. In this contribution, we report on the first results and experience with the Neutron Microscope externally, at a beamline of another neutron source outside the Swiss Spallation Neutron Source (SINQ). In June 2018, NM has been transported to the Institute Laue-Langevin (ILL) and was successfully installed at the D50 beamline for four days. A gadolinium based Siemens star produced at PSI has been used for the assessment of the spatial resolution. The spatial resolution achieved using the Neutron Microscope at ILL-D50 equalled 4.5 μm. Above that, several high-resolution tomographies of various samples were acquired, of which an illustrative example is presented.

Introduction

High spatial resolution neutron imaging is a fast developing area driven by the demands from the user community (for example that of electrochemistry [1]). Provided that ‘high resolution neutron imaging’ is loosely defined as neutron imaging with the capability to resolve about 10 μm structures or better, there are several approaches that demonstrate such capability [2],[3],[4],[5],[6],[7]. At PSI, high resolution neutron imaging has been advanced with the project ‘Neutron Microscope’. In this project, a detector based on a high-numerical aperture objective [8] combined with very thin, though efficient, isotopically-enriched 157-gadolinium oxysulfide scintillator screens [9] was developed and led to the achievement of about five μm isotropic spatial resolution in 2D [10].

Despite these clear advances in the field of the high spatial resolution neutron imaging detectors, it is the available flux (even at rather powerful neutron sources) that sets limitations on both the achievable resolution and the performable experiments. Grosse & Kardjilov [11] have recently proposed a useful theoretical model that estimates the time necessary for neutron radiography/tomography to reveal unambiguously structures with a given contrast at a specific required spatial resolution. Even though the model seems to provide a conservative estimate [12], it is clear that -for certain contrast conditions- neutron tomography of very high spatial resolution requires prohibitively long exposure times even at sources as powerful as SINQ, PSI.

Even for favourable contrast conditions, such as in the case of the neutron tomography of a small porous gold sample [13], the exposure times of several days are required at BOA beamline [14] to achieve approximately $10\text{ }\mu\text{m}$ true spatial resolution in 3D. It is therefore clear that the high spatial resolution neutron imaging applications are bound to seek the highest neutron flux sources.

As the NM has been designed as self-contained detector that can be transported between the beamlines at PSI with only moderate effort, it can also be moved to other neutron sources. Because the neutron source of ILL provides outstanding neutron flux conditions, the NM detector system was transferred recently from PSI to the D50 beamline [15] at ILL and its performance under cutting edge flux conditions has been tested. With an estimated neutron flux of $6 \times 10^9\text{ n/cm}^2\text{s}^{-1}$, the D50 beamline provides currently the highest available flux of cold neutrons for imaging applications. In the following we provide some results of this initial campaign.

Installation of NM at ILL-D50

The entire ‘Neutron Microscope’ instrumentation has been transported to and installed at ILL within one day. The NM has been installed at the most downstream position inside the current D50 beamline bunker (as shown in Figures 1a and 1b).



Figure 1 – PSI ‘Neutron Microscope’ at ILL-D50 beamline: (a) being installed through the open roof into the bunker, (b) positioned at the most downstream position of the ILL-D50, (c) fitted with B_4C sheets and other borated shielding materials. The red dashed arrow in Figure 2b indicates the neutron beam.

It is worth noting that the installation had, despite the independent control of the system, taken only about 6 hours, after which the NM was ready for the first images to be acquired. A significant part of the installation time has been spent on fitting the NM with shielding material (see Figure 1c) in order to avoid activation. The scintillator screen of the NM has been positioned at 11.13 m downstream the 30 mm-diameter pinhole, thus providing collimation ratio

of 371. In the next step of the installation, the NM has been focused using a standard resolution test object - a gadolinium-based Siemens star [16]. The focusing procedure was relatively quick again due to the superior neutron flux.

Results

In the first experiment, to establish the resolution capability achieved, eighty images of the Siemens star pattern, fifty open beam images and ten dark current images were acquired. All images were recorded with 30 seconds exposure time and the test object was positioned in the close vicinity of the scintillator screen (scintillator-sample distance smaller than 0.5 mm). The scintillator was an approximately 3.5 micrometres thick ^{157}Gd isotopically-enriched gadolinium oxysulfide screen. The substrate of the screen consisted of a silicon wafer coated with a 200-nm iridium layer for light output enhancement [17]. The images were acquired using a sCMOS camera (Hamamatsu ORCA Flash 4.0, pixel size 6.5 μm). Thanks to the 5-fold magnification of the NM optics, the pixel size (pixel resolution) of the acquired images was equal to 1.3 micrometers. Two separate open-beam corrected images based on 40 individual radiographs of the test object each were created. These were used for Fourier ring correlation and for the visual inspection of the achieved spatial resolution. One of these images is shown in Figure 2 (left) while the right hand side image presents an enlarged image of the Siemens star centre.

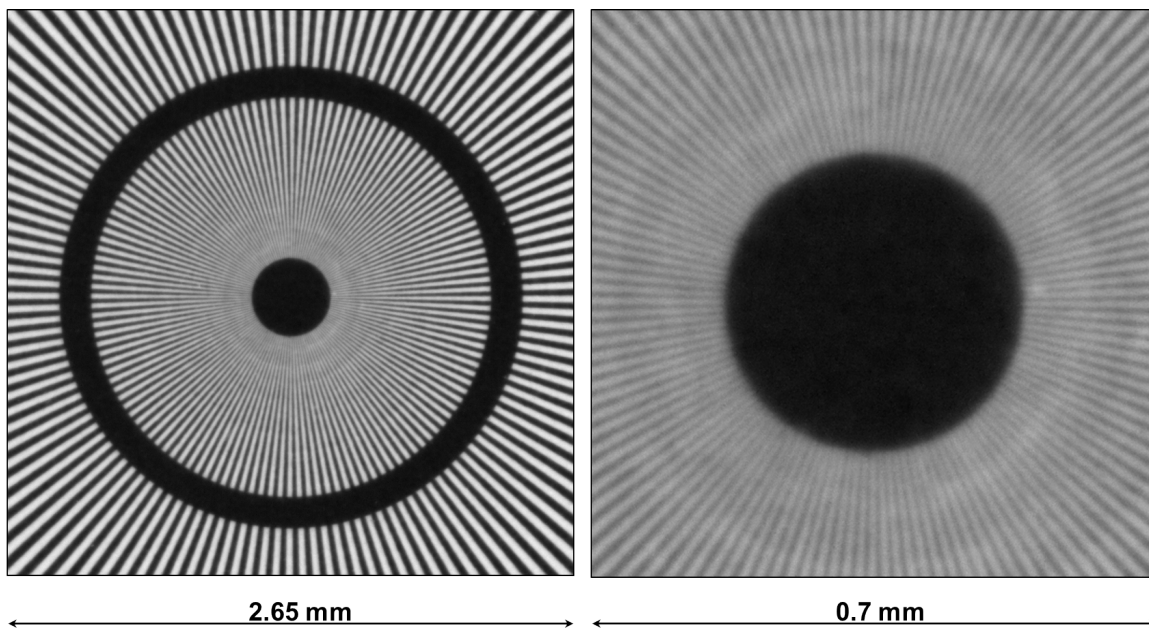


Figure 2 – (left) Neutron radiography of a Gd based Siemens star, (right) close-up of the centre of the Siemens star of the left hand side image clearly revealing the ends of the individual 4.5 micrometres spokes.

It is clearly visible that the thinnest ends of the individual spokes of the Siemens star can be resolved in the image, in particular in the magnified detail on the right hand side of Fig. 2. The size of the thinnest spokes is equal to 4.5 μm (line pair: 9 μm). For the quantitative analyses, Fourier ring correlation [18] was applied to the Siemens star images and resulted in a measured spatial resolution of 4.2 μm .

Subsequently, after assessing the resolution experimentally, several small static samples were tomographed. The tomographed samples included pieces of Zircaloy nuclear fuel cladding [19], bits of additively manufactured gold alloys, and a cylinder of a diameter of approximately 2.5 mm of a gold-lead alloy.

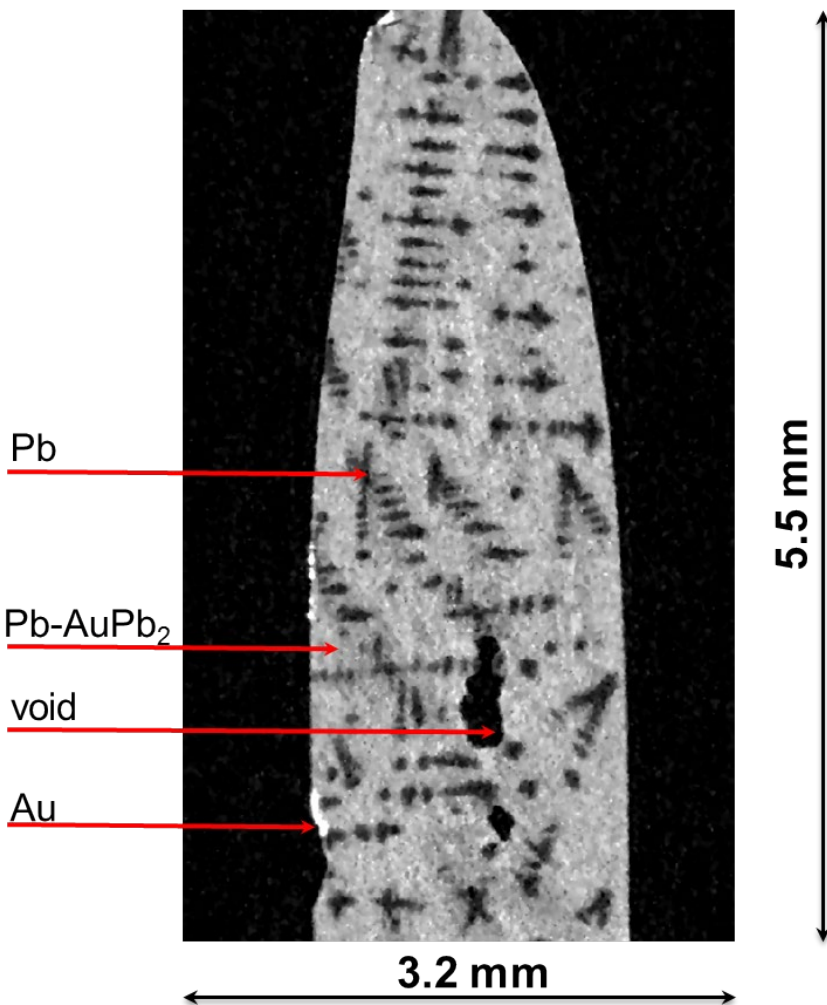


Figure 3 – Example of a neutron microtomography using the PSI 'Neutron Microscope' at the ILL-D50 beamline: A vertical slice from a neutron microtomography dataset showing dendritic microstructures of lead, voids and gold in a sample of a gold-lead alloy.

The detailed description of the results of these neutron microtomographies goes beyond the purpose and the scope of this paper. However, Figure 3 provides an example of the high quality of the resulting datasets showing a randomly chosen vertical slice from the microtomographic dataset revealing in detail the dendritic microstructure of lead in a gold-lead alloy [20] with unprecedented spatial resolution. From the point of view of the temporal resolution, the presented lead-gold alloy microtomography required approximately 12 hours of beamtime only - including the acquisition of open beam, dark current and black body [21] images.

Discussion & Outlook

From the practical and logistic point of view, the installation of NM at ILL was a rather swift procedure. One of the issues that need to be addressed when using a detector at another neutron facility is the activation of the system. Naturally, the pieces of NM that were exposed to the direct beam (i.e. scintillator screen/holder and the mirror) were expected to be activated beyond a level for immediate release. However, readily available duplicates of these pieces enable transfer and usability of the system elsewhere within about 24-48 hours.

Despite taking care with shielding the NM from any unnecessary other neutrons, few parts of the rest of the instrumentation were very slightly activated (likely due to neutrons scattered from

the sample/scintillator/mirror) at the end of the campaign ($\sim 0.15 \mu\text{Sv/h}$). This activation led to the necessity to prolong the stay of NM at ILL for another 24 hours. The procurement of more efficient shielding for NM can alleviate this situation in the future.

Regarding the results themselves, it was shown that the favourable combination of NM with the superior flux at ILL-D50 can provide highest spatial resolution and quality of neutron imaging data both in 2D and in 3D with significantly reduced exposure times and hence higher efficiency. It can be concluded that highest resolution imaging capabilities at ILL are highly desirable for the neutron imaging community. This could enable not only a higher throughput of samples with scanning requirements at highest currently achievable resolutions as demonstrated in this contribution, but also achieving better than current temporal resolutions in time-resolved studies [22],[23]. In addition, there appears to be still room for (i) further pushing the spatial resolution limit towards even closer to $1 \mu\text{m}$ and (ii) combination of the detector with neutron optics (e.g. [24]).

Summary

PSI ‘Neutron Microscope’ was successfully installed and tested at ILL-D50 beamline in Grenoble for 4 days. The visual assessment and the Fourier ring correlation criterion of the images of the standard resolution test pattern (PSI gadolinium Siemens star) resulted in a measured spatial resolution better than $4.5 \mu\text{m}$. Also, several high-resolution tomographies of relevant static samples were acquired within the available allocated beamtime window. They demonstrated the highest resolution neutron microtomography and underlined the capability of the fast measurements at extreme spatial resolutions at ILL-D50 with the NM technology developed at PSI.

Acknowledgement

Dariusz Gawryluk, Marc Raventós, Eric Ricardo Carreon and Marisa Medarde (all PSI) are kindly thanked for the provision of the gold-lead alloy sample.

References

- [1] P. Boillat, E. H. Lehmann, P. Trtik, and M. Cochet, “Neutron imaging of fuel cells – Recent trends and future prospects,” *Curr. Opin. Electrochem.*, vol. 5, no. 1, 2017. <https://doi.org/10.1016/j.coelec.2017.07.012>
- [2] F. Krejci *et al.*, “Development and characterization of high-resolution neutron pixel detectors based on Timepix read-out chips,” *J. Instrum.*, vol. 11, no. 12, 2016. <https://doi.org/10.1088/1748-0221/11/12/C12026>
- [3] A. Faenov *et al.*, “Lithium fluoride crystal as a novel high dynamic neutron imaging detector with microns scale spatial resolution,” *Phys. Status Solidi Curr. Top. Solid State Phys.*, vol. 9, no. 12, 2012. <https://doi.org/10.1002/pssc.201200185>
- [4] A. S. Tremsin *et al.*, “High resolution neutron imaging capabilities at BOA beamline at Paul Scherrer Institut,” *Nucl. Instruments Methods Phys. Res. Sect. A Accel. Spectrometers, Detect. Assoc. Equip.*, vol. 784, 2015. <https://doi.org/10.1016/j.nima.2014.09.026>
- [5] S. H. Williams *et al.*, “Detection system for microimaging with neutrons,” *J. Instrum.*, vol. 7, no. 2, 2012. <https://doi.org/10.1088/1748-0221/7/02/P02014>
- [6] D. S. Hussey, J. M. LaManna, E. Baltic, and D. L. Jacobson, “Neutron imaging detector with $2 \mu\text{m}$ spatial resolution based on event reconstruction of neutron capture in gadolinium oxysulfide scintillators,” *Nucl. Instruments Methods Phys. Res. Sect. A Accel. Spectrometers, Detect. Assoc. Equip.*, 2017. <https://doi.org/10.1016/j.nima.2017.05.035>
- [7] M. Morgano, P. Trtik, M. Meyer, E. H. Lehmann, J. Hovind, and M. Strobl, “Unlocking high spatial resolution in neutron imaging through an add-on fibre optics taper,” *Opt. Express*, vol. 26, no. 2, 2018. <https://doi.org/10.1364/OE.26.001809>
- [8] P. Trtik *et al.*, “Improving the Spatial Resolution of Neutron Imaging at Paul Scherrer Institut

- The Neutron Microscope Project,” in *Physics Procedia*, 2015, vol. 69. <https://doi.org/10.1016/j.phpro.2015.07.024>
- [9] P. Trtik and E. H. Lehmann, “Isotopically-enriched gadolinium-157 oxysulfide scintillator screens for the high-resolution neutron imaging,” *Nucl. Instruments Methods Phys. Res. Sect. A Accel. Spectrometers, Detect. Assoc. Equip.*, vol. 788, 2015. <https://doi.org/10.1016/j.nima.2015.03.076>
- [10] P. Trtik and E. H. Lehmann, “Progress in High-resolution Neutron Imaging at the Paul Scherrer Institut-The Neutron Microscope Project,” *J. Phys. Conf. Ser.*, vol. 746, no. 1, 2016. <https://doi.org/10.1088/1742-6596/746/1/012004>
- [11] M. Grosse and N. Kardjilov, “Which Resolution can be Achieved in Practice in Neutron Imaging Experiments? - A General View and Application on the Zr - ZrH₂and ZrO₂- ZrN Systems,” in *Physics Procedia*, 2017. <https://doi.org/10.1016/j.phpro.2017.06.037>
- [12] M. Grosse, P. Trtik, and B. Schillinger, in preparation
- [13] P. Trtik, “Neutron microtomography of voids in gold,” *MethodsX*, vol. 4, 2017. <https://doi.org/10.1016/j.mex.2017.11.009>
- [14] M. Morgan, S. Peetermans, E. H. Lehmann, T. Panzner, and U. Filges, “Neutron imaging options at the BOA beamline at Paul Scherrer Institut,” *Nucl. Instruments Methods Phys. Res. Sect. A Accel. Spectrometers, Detect. Assoc. Equip.*, vol. 754, pp. 46–56, 2014. <https://doi.org/10.1016/j.nima.2014.03.055>
- [15] D. Dauti, A. Tengattini, S. Dal Pont, N. Toropovs, M. Briffaut, and B. Weber, “Analysis of moisture migration in concrete at high temperature through in-situ neutron tomography,” *Cem. Concr. Res.*, no. 111, pp. 41–55, 2018. <https://doi.org/10.1016/j.cemconres.2018.06.010>
- [16] C. Grünzweig, G. Frei, E. Lehmann, G. Kühne, and C. David, “Highly absorbing gadolinium test device to characterize the performance of neutron imaging detector systems,” *Rev. Sci. Instrum.*, vol. 78, no. 5, 2007. <https://doi.org/10.1063/1.2736892>
- [17] J. Crha, “Light Yield Enhancement of 157-Gadolinium Oxysulfide Scintillator Screens for the High-Resolution Neutron Imaging,” *MehtodsX*, vol. 6., pp. 107-114. <https://doi.org/10.1016/j.mex.2018.12.005>
- [18] M. Van Heel and M. Schatz, “Fourier shell correlation threshold criteria,” *J. Struct. Biol.*, vol. 151, no. 3, 2005. <https://doi.org/10.1016/j.jsb.2005.05.009>
- [19] W. Gong, P. Trtik, S. Valance, and J. Bertsch, “Hydrogen diffusion under stress in Zircaloy: High-resolution neutron radiography and finite element modeling,” *J. Nucl. Mater.*, vol. 508, pp. 459–464, 2018. <https://doi.org/10.1016/j.jnucmat.2018.05.079>
- [20] M. Medarde *et al.*, “Lead–gold eutectic: An alternative liquid target material candidate for high power spallation neutron sources,” *J. Nucl. Mater.*, vol. 411, no. 1, pp. 72–82, 2011. <https://doi.org/10.1016/j.jnucmat.2011.01.034>
- [21] P. Boillat *et al.*, “Chasing quantitative biases in neutron imaging with scintillator-camera detectors: A practical method with black body grids,” *Opt. Express*, vol. 26, no. 12, 2018. <https://doi.org/10.1364/OE.26.015769>
- [22] P. Trtik *et al.*, “Release of internal curing water from lightweight aggregates in cement paste investigated by neutron and X-ray tomography,” *Nucl. Instruments Methods Phys. Res. Sect. A Accel. Spectrometers, Detect. Assoc. Equip.*, vol. 651, no. 1, 2011. <https://doi.org/10.1016/j.nima.2011.02.012>
- [23] J. Terreni *et al.*, “Observing Chemical Reactions by Time-Resolved High-Resolution Neutron Imaging,” *J. Phys. Chem. C*, vol. 122, no. 41, pp. 23574–23581, 2018. <https://doi.org/10.1021/acs.jpcc.8b07321>
- [24] M. Yamada *et al.*, “Pulsed neutron-beam focusing by modulating a permanent-magnet sextupole lens”, *Progress Theoret Experim Phys.* no. 4, 2015, 043G01. <https://doi.org/10.1093/ptep/ptv015>